

Dynamic Network Topology Portrait for Digital Twin Optical Network

Yonghan Wu^{ID}, Min Zhang, Lifang Zhang^{ID}, Jin Li^{ID}, Xue Chen^{ID}, Member, IEEE,
and Danshi Wang^{ID}, Member, IEEE

Abstract—Digital twin (DT) as one promising technology has been introduced in optical networks, whose role is to achieve interactive functions and intelligent control by building a bridge between physical space and digital space. In this paper, a multifactor-associated network topology portrait (NTP) scheme is proposed to draw a dynamic, real-time, and comprehensive topology representation for DT optical network (DTON). Multiple parameters from nodes and links are jointly evaluated, including link distance, link loss, optical signal-to-noise ratio, bandwidth utilization rate, load capacity, node failure rate, and link failure rate, involving both network layer and physical layer. Based on the NTP, the performance of dynamic routing computation combined with six different routing algorithms is studied. Here, the time for routing computation is sacrificed a little bit in exchange for significant improvements in outage probability, outage latency, and the number of service requests.

Index Terms—Digital twin optical network, network topology representation, multi-factor evaluation, routing computation.

I. INTRODUCTION

DIGITAL twin (DT) has emerged as a promising technology for bridging the connection gap between physical spaces and digital spaces, which is one of the most important enabling technologies for Industry 4.0 [1]. Recently, DT has also been introduced in the telecommunications fields, from mobile networks [2] to optical networks [3]. The concept of DT optical network (DTON) was proposed in [3], and an architecture of DTON was presented in [4] based on the virtual replica of the physical optical network in a digital manner for the simulation of specific behaviors before actual implementation. However, the existing optical communication systems and networks encounter severe

challenges in the accurate monitoring, online management, real-time control, and rapid maintenance. The conditions of the physical layer are ideal, stable, and static. It has limited sensing and modeling capabilities, and can only detect the power and signal to noise ratio. Moreover, in network layer, the traditional optical network can only describe the static and simple network topology, and cannot realize the whole function from physical layer to network layer. Compared with traditional optical network, DTON can add significant value to the planning and operational phases of optical networks by predicting network incidents accurately, simulating different scenarios dynamically, and providing optimization strategies timely. DTON is envisioned to pave the way for close monitoring, high-fidelity modeling, real-time interaction, and dynamic network orchestration for autonomous optical networks. Accordingly, several applications of DTON have been preliminarily explored, including soft-failure location [5], quality of transmission (QoT) estimation [6], optical power control [7], amplifier gain prediction [8], and transceiver configuration [9]. However, these schemes mainly focused on the physical entities or end-to-end transmission system from the perspective of physical layer but losing sight of network layer.

In DTON, the network layer is a key component for global control and management [10], [11]. In the network layer, one of the primary tasks for DTON is to establish the mirror model of network topology (NT) to characterize the comprehensive network structure and status information, which is significant for dynamic routing computing [12], flexible resource allocation [13], [14], and accurate traffic prediction [15]. The dynamic scenarios and elastic cases are also significant in network layer. For example, dynamic routing and spectrum allocation in elastic optical network also puts forward higher requirements for the dynamics scenarios [16]. In addition, the technologies for realizing highly efficient data migration and backup for Big Data applications in elastic optical inter-data-center (inter-DC) networks is a hot topic [17]. Meanwhile, how to optimize service function chains (SFC) deployment and readjustment in the dynamic situation is closely related to user experience [18]. DTON may provide solutions for both dynamic scenarios and elastic cases, especially in the description of the network topology. To establish the mirror model for the network topology, it is necessary to put forward a comprehensive scheme for the description of the topology, which can depict the physical structure the network topology and characterize the logical relationship containing the information of network status and system condition. In optical networks, several network topology description (NTD) schemes

Manuscript received 19 September 2022; revised 27 December 2022; accepted 28 January 2023. Date of publication 31 January 2023; date of current version 16 May 2023. This work was supported in part by the National Natural Science Foundation of China under Grants 61975020 and 62171053, and in part by the National Key R&D Program of China under Grant 2022YFB2901100. (Corresponding authors: Min Zhang; Danshi Wang.)

Yonghan Wu, Min Zhang, Jin Li, Xue Chen, and Danshi Wang are with the State Key Laboratory of Information Photonics and Optical Communications, Beijing University of Posts and Telecommunications, Beijing 100876, China (e-mail: kevinwu1666@bupt.edu.cn; mzhang@bupt.edu.cn; jinli@bupt.edu.cn; xuechen@bupt.edu.cn; danshi_wang@bupt.edu.cn).

Lifang Zhang is with the China Unicom, the Intelligent Network Innovation Center of Chinaunicom, Beijing 100033, China (e-mail: zhanglf49@chinaunicom.cn).

Color versions of one or more figures in this article are available at <https://doi.org/10.1109/JLT.2023.3241187>.

Digital Object Identifier 10.1109/JLT.2023.3241187

have been proposed by evaluating different network factors such as the layered graph model based on routing and the wavelength assignment (RWA) model [19], inter-node connectivity as well as detailed node and overall network configurations in the form of netlist files [20], intra-node structures as well as inter-node fiber connections with different switching functionalities of individual optical components based on integer linear programming (ILP) formulas [21]. However, these NTD schemes are fundamentally represented in the form of static graphs or netlists, they only considering the graphical representation or network configurations in terms of simple factors. Consequently, these methods are limited in terms of providing the complete topological information and are incapable of characterizing the dynamic network scenarios. DTON establishes a high demand for topology model with capabilities of dynamic, real-time, and comprehensive description. To describe the network topology more comprehensively and clearly, both the parameters from the physical layer (like optical signal-to-noise ratio (OSNR) [22] and transmission loss [23]) and the factors from the network layer (like bandwidth utilization rate [24] and traffic rating [25]) need to be considered simultaneously.

In this paper, a multifactor-associated network topology portrait (NTP) scheme is proposed to draw a dynamic, real-time, and comprehensive topology representation for DTON. Both the connections between the nodes and multiple parameters are jointly evaluated, including link distance, link loss, OSNR, bandwidth utilization rate, load capacity, node failure rate, and link failure rate, involving the network and physical layers. The connections between nodes are represented by a two-dimensional matrix involving all pairs of connected nodes and the measured distance of links between them in a physical network topology. In addition, some parameters are not included in the modeling scheme but associated with performance parameters above, such as transmission delay of links and processing delay of nodes. Transmission delay is affected by link distance. The processing delay of nodes is related to traffic rate and node failure rate. Therefore, the parameters above are representative and the scheme of the NTP is reasonable. The multiple parameters in network topology, including nodes parameters and links parameters, are evaluated based on data normalization and the linear weighted method. Based on the NTP, the performance of dynamic routing computation combined with six different routing algorithms is studied. It is proved that the NTP based on multi-factor evaluation ensures the comprehensiveness and globality of network topology. In dynamic routing computation, although the routing computation time increases slightly, the performances of routing computation in terms of the outage probability, outage latency, and the number of service requests are remarkably improved.

II. PRINCIPLES OF THE NETWORK TOPOLOGY PORTRAIT

The principle of the proposed NTP is illustrated in Fig. 1. First, the NTP is composed of four key parts: network topology, topology portrait, DT modeling, and monitoring & feedback system.

Network topology comprises the graphic description and topological parameters. Graphic description explains the connection between nodes and links; topological parameters represent the parameters of nodes and links. For nodes, five parameters are considered, involving geographic location, load capacity, traffic rating, node failure rate, and connectivity. Geographical location of nodes is defined using the distance from the point to the center of the circle. Connectivity is considered as the number of links on nodes. Load capacity represents the load status of nodes [26]. Traffic rating is influenced by the single-wavelength rates. Node failure rate corresponds to the failure probability of a node during service transmission [27]. For links, five more parameters are considered, including the link distance, transmission loss, OSNR, link failure rate, and bandwidth utilization rate. The link distance is converted into the straight-line distance between any two nodes. The transmission loss is directly proportional to the link distance. OSNR is closely related to the fiber link length and amplifier amount. The definition of link failure rate is similar to the node failure rate indicating the probability of a link failure at a certain point in time during service transmission [28]. The bandwidth utilization rate is defined as the bandwidth usage of links.

In DT modeling, the graphic data and performance parameters of the network topology are converted into graphic matrix and comprehensive evaluation under multiple factors through graphic modeling and multi-mapping modeling, respectively. All the evaluation above are integrated into comprehensive evaluation of nodes and links after data normalization [29] and linear weighting [30]. The comprehensive evaluation are quantified and scored from 60 to 100 and divided into different grades. According to the evaluation scores, all the nodes are ranked into five levels (excellent, good, ordinary, bad, and worse) and links are ranked into four levels (excellent, good, normal, and bad). For nodes, five levels correspond to five numerical intervals, including [60,68), [68,76), [76,84), [84,92) and [92,100]. Similarly, for links, four levels correspond to four numerical intervals, including [60,70), [70,80), [80,90) and [90,100]. Accordingly, the nodes or links with higher evaluation grade are preferentially selected for specific tasks such as routing computation. Herein, different levels are visualized in different colors, such that the topology portrait can be presented intuitively and vividly by integrating the multifactor-associated evaluation into the graphic matrix. In dynamic scenarios, the monitoring & feedback system enables the topology portrait to be adjusted in real time based on monitoring of the change of parameters from network topology.

With the aid of the topology portrait in DTON, the solutions for the accident of network topology as well as adjustments can be provided for different tasks, such as routing computation, traffic prediction, load balancing, or resource allocation. Accordingly, the optimization strategy and control action are fed back to the network system. Here, along with routing computation, the NTP construction details involving five parts, namely graphic modeling of NTP, parameters modeling for NTP, data normalization and comprehensive evaluation for nodes and links, routing algorithms, and monitoring & feedback system are also presented.

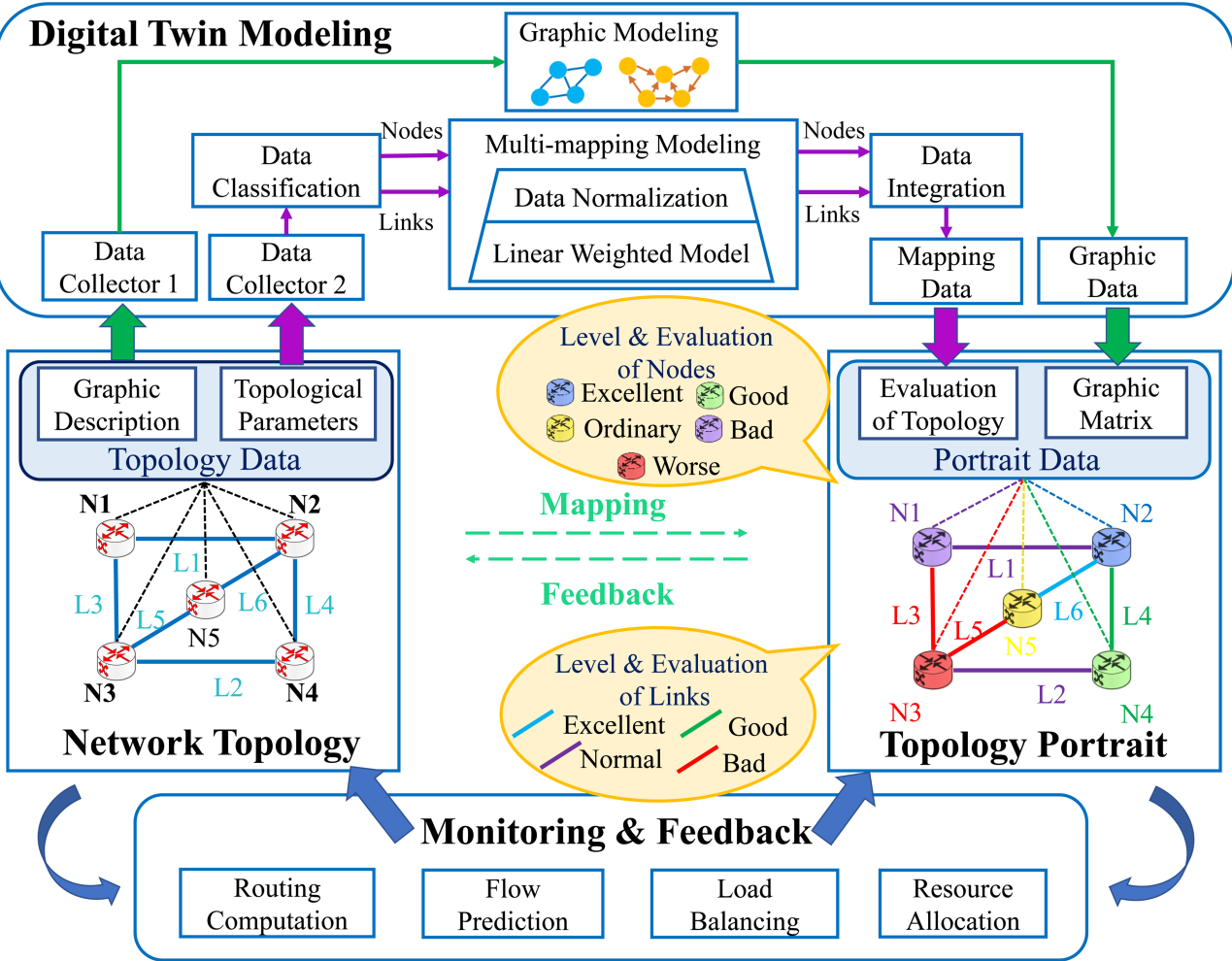


Fig. 1. Principle and schematic of multifactor-associated NTP in DTON, involving network topology, topology portrait, digital twin modeling, and monitoring & feedback. The topology portrait is the mirror model of network topology. Digital twin modeling is responsible for establishing NTP Monitoring & feedback is realize dynamic monitoring and interaction between network topology and NTP.

A. Graphic Modeling of NTP

The network topology is defined as an undirected graph $G(V, E)$, where V and E are the aggregation of nodes and links. $G(V, E)$ is designed to provide a basic graphical support for NTP in DTON. Each node and link corresponds to $v_i \in V$ ($i \in [1, u]$) and $e_j \in E$ ($j \in [1, v]$), where u and v correspond to the number of nodes and links. The schematic of the graphic description in NTP is illustrated in Fig. 2, considering the network topology with 7 nodes and 10 links as an example.

Based on the undirected graph, the graphic matrix is defined as G , as denoted by (1), where the serial number of each node and link correspond to n_i ($i \in [1, u]$) and l_k ($k \in [1, v]$). The measured distance of each link is defined as ld_k ($k \in [1, v]$).

$$G = \begin{bmatrix} n_1 & n_2 & l_1 & ld_1 \\ \dots & \dots & \dots & \dots \\ n_i & n_j & l_k & ld_k \\ \dots & \dots & \dots & \dots \\ n_{u-1} & n_u & l_v & ld_v \end{bmatrix} \quad (1)$$

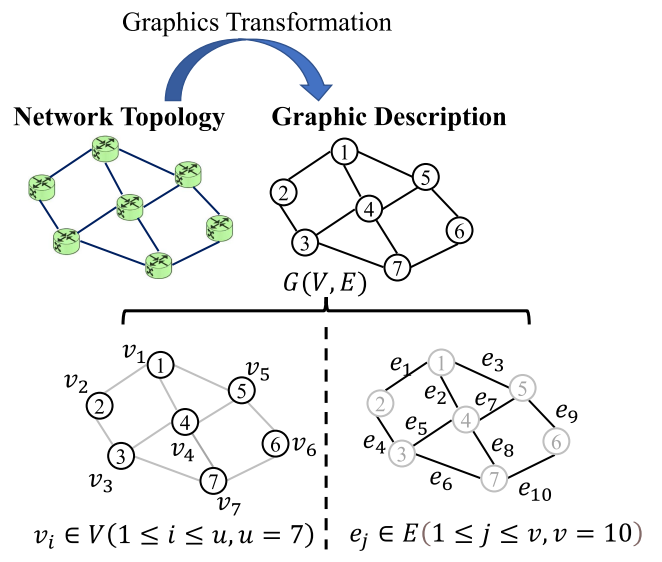


Fig. 2. Graphical description of the network topology.

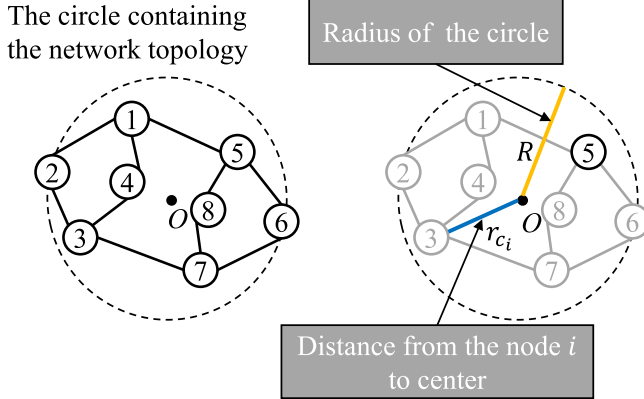


Fig. 3. Schematic of the centrality of geographical location for nodes.

By constructing the graph matrix G , the basic elements such as the number of nodes and links, the labels of nodes and links, and the connection relations in network topology are mapped into a graphic representation. Next, the modeling and analysis of the parameters of nodes and links in the topology will be conducted.

B. Parametric Model for NTP

The topological parameters characterizing the performance of nodes and links are described in detail to provide clearer and more comprehensive information to the NTP. The parametric model comprises node parameters and link parameters, corresponding to the descriptions of nodes and links, respectively. The purpose of parametric model is to provide richer and more comprehensive description for NTP in DTON.

For nodes, the parameters are divided into five parts, involving geographic location, load capacity, traffic rating, node failure rate, and connectivity. First, to evaluate the geographical location of nodes, the definition of the distance from the point to the center of the circle is introduced, aiming to enrich the NTP in terms of nodes with the geographical characteristics for DTON. The circle containing all nodes and links in the network topology is shown in Fig. 3, wherein radius R is half of the distance between the two farthest nodes in the topology, and the distance from the node i to the center is defined as r_{ci} , and R_c corresponds to the set of r_{ci} satisfying $r_{ci} \in R_c$ ($i \in [1, u]$).

The centrality of geographical location of the node i is defined as nc_i , as illustrated by (2), where the set of nc_i is N_c , satisfying $nc_i \in N_c$ ($i \in [1, u]$).

$$nc_i = \frac{2R - r_{ci}}{R} \quad (2)$$

The value of nc_i satisfies $nc_i \in [1, 2]$. The larger the value of nc_i , the closer the distance between the node i and the center of the topology, and the stronger is the centrality of the node i . The smaller the value of nc_i , the weaker is the centrality of the node i . nc_i equal to 1 implies that the node i is at the boundary of the topology, and the value equals to 2 implies the node i is at the topology center.

On the basis of the centrality of the geographical location of nodes, the connectivity of nodes is considered as another aspect of the geographic feature of nodes. When the network topology is described as a directed graph, the connectivity of the node i is defined as con_i , as denoted by (3), where the set of con_i is Con , satisfying $con_i \in Con$ ($i \in [1, u]$). Among them, id_i and od_i represent the in-degree and the out-degree [31] of the node i , respectively. On the contrary, when the network topology is described as an undirected graph, the in-degree and the out-degree of nodes are no longer considered, and con_i of the node i is considered as the number of links on the node.

$$con_i = id_i + od_i \quad (3)$$

To provide the descriptions of network performance for nodes in NTP, the definition of traffic rating, load capacity and node failure rate are proposed. The increasing of single-wavelength rates provides larger capacity for service transmission in optical network, and further significantly improve the traffic rating [32]. Accordingly, the single-wavelength rates can be used to characterize the traffic rating. The traffic rating of nodes is divided into four levels, referring to the conception of the single-wavelength rates of nodes [32]. The single-wavelength rates are divided into four different levels, corresponding to 100 Gbit/s, 200 Gbit/s, 400 Gbit/s, and 800 Gbit/s. The traffic rating and the single-wavelength rates of the node i are defined as tr_i and sr_i , respectively, and the relation between them satisfies (4), where the numbers from 1 to 4 indicate different levels. The set of tr_i is Tr , satisfying $tr_i \in Tr$ ($i \in [1, u]$), and the set of sr_i is Sr , satisfying $sr_i \in Sr$ ($i \in [1, u]$).

$$tr_i = \begin{cases} 1, & \text{if } sr_i = 800 \text{ Gbit/s} \\ 2, & \text{if } sr_i = 400 \text{ Gbit/s} \\ 3, & \text{if } sr_i = 200 \text{ Gbit/s} \\ 4, & \text{if } sr_i = 100 \text{ Gbit/s} \end{cases} \quad (4)$$

The load capacity represents the load status of nodes, indicating the maximum volume of service requests of nodes [33], and the load capacity of the node i is defined as lc_i , where the set of lc_i is Lc , satisfying $lc_i \in Lc$ ($i \in [1, u]$).

The node failure rate of the node i is defined as nf_i , where the set of nf_i is Nf , satisfying $nf_i \in Nf$ ($i \in [1, u]$). The threshold of node failure rate is defined as Nft . The relation between nf_i and Nft is defined as (5):

$$nf_i = \begin{cases} 0, & \text{if } nf_i \leq Nft \\ nf_i, & \text{if } nf_i > Nft \end{cases} \quad (5)$$

Further, DTON still needs the description of links, especially in NTP. For the links, the parameters are also divided into five parts, involving the link distance, transmission loss, OSNR, link failure rate, and bandwidth utilization rate. The link distance complements the graphical description of the NTP, and the other four aspects is to map the performance parameters of links into NTP.

First, referring to the measured distance between any two nodes, the link distance is converted into the actual straight-line distance between any two nodes. The link between the node i and the node j is defined as the link k ($k \in [1, v]$). The measured distance of the link k is ld_k , referring to the graphic modeling

of the NTP. Accordingly, the actual straight-line distance of the link k is defined as d_k , as (6), where the constant m represents the proportionality coefficient referring to the scale that relates the measured distance to the actual distance. The set of d_k is D , satisfying $d_k \in D$ ($k \in [1, v]$).

$$d_k = m \cdot ld_k \quad (6)$$

The transmission loss of the link k is defined as tl_k , where the set of tl_k is Dl , satisfying $tl_k \in Tl$ ($k \in [1, v]$). Meanwhile, tl_k and d_k are directly proportional, as (7), and the proportionality coefficient between them is a namely fiber attenuation coefficient [34], which implies that the greater the link distance, the greater the transmission loss. The value of a satisfying $a = 0.2$ dB/km refers to the loss coefficient of 1550 nm for a single-mode fiber [34].

$$tl_k = a \cdot d_k \quad (7)$$

For OSNR, generally, it is closely related to the link length and amplifier amount. Normally, the range for OSNR is 10 dB to 30 dB. The OSNR of the link k is defined as $osnr_k$, where the set of $osnr_k$ is $OSNR$, satisfying $osnr_k \in OSNR$ ($k \in [1, v]$). For the convenience of calculation, in this study, the value of $osnr_k$ is temporarily set as a random number ranging from 10 dB to 30 dB:

$$osnr_k = \{x | 10 \leq x \leq 30\} \quad (8)$$

The definition of the link failure rate is similar to the node failure rate which indicates the probability of a link failure at a time during the process of service transmission. The link failure rate of the link k is defined as lf_k , where the set of lf_k is Lf , satisfying $lf_k \in Lf$ ($k \in [1, v]$). The threshold of the node failure rate is defined as Lft . The relation between lf_k and Lft is expressed in (9).

$$lf_k = \begin{cases} 0, & \text{if } lf_k \leq Lft \\ lf_k, & \text{if } lf_k > Lft \end{cases} \quad (9)$$

The bandwidth utilization rate on the link k is defined as br_k , where the set of br_k is Br , satisfying $br_k \in Br$ ($k \in [1, v]$). The bandwidth utilization rate is 30% to 80%. When the bandwidth utilization rates is 30%, the performance of service transmission is favorable. The bandwidth utilization rates is 80% means the network is greatly congested. Here, the value of br_k of the link k is temporarily set as a random number ranging from 30% to 80% dB:

$$br_k = \{x | 30\% \leq x \leq 80\%\} \quad (10)$$

As mentioned above, the multi-parameter modeling analysis of nodes and links has been preliminarily completed. In the next section, the data of parameters are normalized with different dimensions and complete comprehensive evaluation of nodes and links.

C. Data Normalization and Comprehensive Evaluation for Multi-Parameter Nodes and Links

In order to complete the comprehensive evaluation of the above parameters and further provide comprehensive evaluation

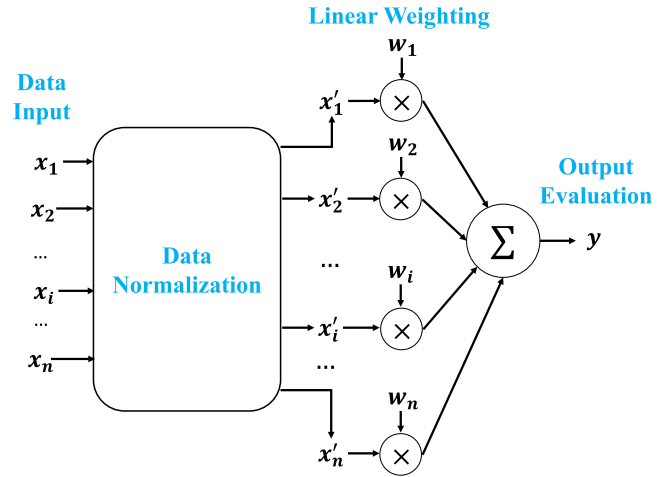


Fig. 4. Process of data normalization and linear weighting method.

and the level in terms of nodes and links for NTP in DTOM, the methods of data normalization and multi-factor evaluation are introduced. The function of data normalization is to remove the unit of measurement of the data, and the processed data can be further used for analysis and integration. In this work, because multiple factors in the network need to be linearly weighted and comprehensively evaluated, the data with different units are required to be normalized in advance. The process of analysis for comprehensive evaluation is illustrated in Fig. 4, where n and x_i indicate the number of parameter types and the evaluation of certain types of parameters from nodes or links, and i satisfies $i \in [1, n]$. Through the data normalization operation on the input data, the parameters are unified in dimension, and x_i is converted to x'_i . Subsequently, the normalized data are linearly weighted with their respective weights:

$$x = \sum_{i=1}^n w_i x_i \quad (11)$$

Here, w_i and y represent the weight of x_i and comprehensive evaluation.

There are many approaches to normalize data involving Min-Max standardization, Z-score standardization, and nonlinear normalization [35], [36]. Nonlinear normalization involves log normalization and trigonometric normalization. In this paper, four data normalization methods which are the most common used methods are selected, including Min-Max standardization, ratio normalization, log normalization, and trigonometric normalization [36]. As (12), $f_m(x)$, $f_d(x)$, $f_l(x)$, and $f_t(x)$ correspond to the four normalization methods mentioned above. x_{\min} and x_{\max} represent the maximum and minimum value of the variable x . The base of the logarithm is 10. X_{sum} represents the sum of x . Based on (12), referring to the student evaluation system [37], the normalized parameter data whose value ranges from 0 to 1 is converted to 60 to 100, which is used for an

TABLE I
DESCRIPTIONS OF VARIABLE PARAMETERS IN NTP

| Symbol | Explain | Symbol | Explain | Symbol | Explain |
|---------|--|--------|---|----------|--|
| u | Number of nodes | Sr | Set of sr_i | a | Fiber attenuation coefficient |
| v | Number of links | tr_i | Traffic rating of the node i | $osnr_k$ | OSNR of the link k |
| ld_k | Measured distance of the link k | Tr | Set of tr_i | $OSNR$ | Set of $osnr_k$ |
| R | Radius of circle containing the network topology | lc_i | Load capacity of the node i | lf_k | Link failure rate of the node k |
| rc_i | Distance from the node i to the center of the circle containing network topology | Lc | Set of lc_i | Lf | Set of the node lf_k |
| R_c | Set of rc_i | nfi | Node failure rate of the node i | Lft | Threshold of link failure rate |
| nc_i | Geographical location of the node i | Nf | Set of nfi | br_k | Bandwidth utilization rate on the link k |
| N_c | Set of nc_i | Nft | Threshold of node failure rate | Br | Set of br_k |
| con_i | Connectivity of the node i | d_k | Actual distance of the link k | En_i | Evaluation of the node i |
| Con | Set of con_i | D | Set of d_k | EN | Set of En_i |
| id_i | In-degree of the node i | m | Proportionality coefficient of distance | El_k | Evaluation of the link k |
| od_i | Out-degree of the node i | tl_k | Transmission loss of the link k | El | Set of El_k |
| sr_i | Single-wave rates of the node i | Tl | Set of tl_k | | |

independent evaluation of the parameters.

$$\left\{ \begin{array}{l} f_m(x) = \frac{x - x_{\min}}{x_{\max} - x_{\min}} \\ f_d(x) = \frac{x}{X_{sum}} \\ f_l(x) = \frac{\log_{10}(x)}{\log_{10}(x_{\max})} \\ f_t(x) = \arctan(x) \cdot \frac{2}{\pi} \end{array} \right. \quad (12)$$

Supported by the above description and conceptions, the detailed descriptions of parameters for nodes and links are provided as shown in Table I. For nodes, through data normalization, the five parameters, namely nc_i , con_i , tr_i , lc_i , and nfi are transformed into normalized and unified dimensional data corresponding to nc'_i , con'_i , tr'_i , lc'_i , and nfi'_i , respectively; the set of these parameters corresponds to N'_c , Con' , Tr' , Lc' , and Nf' , respectively. For links, the five parameters, namely d_k , tl_k , $osnr_k$, lf_k , and br_k are transformed into normalized and unified dimensional data corresponding to d'_k , tl'_k , $osnr'_k$, lf'_k , and br'_k , and the set of these parameters corresponds to D' , Tl' , $OSNR'$, Lf' , and Br' , respectively.

Next, the evaluation of nodes and links are shown based on the linear weighting method. The evaluation of the node i is defined as En_i , as shown in (13), where the set of En_i is EN , satisfying $En_i \in EN$ ($i \in [1, u]$).

$$En_i = \omega_1 nc'_i + \omega_2 con'_i + \omega_3 tr'_i + \omega_4 lc'_i + \omega_5 nfi'_i \quad (13)$$

For links, the transmission loss is directly proportional to the link distance. If the two parameters are both contained in

linear weighting, the weights of these factors will become too high and further affect the rationality of the evaluation for links. Therefore, only the link distance is selected as a part of the linear weighting. The evaluation of the link k is defined as El_k in (14), where the set of El_k is EL , satisfying $El_k \in EL$ ($k \in [1, v]$).

$$El_i = \alpha_1 d_k' + \alpha_2 osnr_k' + \alpha_3 lf_k' + \alpha_4 br_k' \quad (14)$$

Here, w_1 , w_2 , w_3 , w_4 , and w_5 correspond to the weights of five parameters from nodes. α_1 , α_2 , α_3 and α_4 correspond to the weights of four parameters selected from the parameters of links. In the beginning, the weight values are preset to be equal. For nodes, the weighting factors named w_i ($i \in [1, 5]$) satisfy $w_i = 0.2$. For links, the weighting factors named α_j ($j \in [1, 4]$) satisfy $\alpha_j = 0.2$. Then, weights will be adjusted according to change of parameter values in dynamic scenarios. In this work, by solving the variance of the data sets corresponding to different parameters, the weight value of each parameter is further determined. Taking five parameters of nodes as an example, we respectively calculate five variances of these parameters after data normalization. We further sum the five variances and calculate the proportion of each variance within the sum. Finally, the proportion of each variance in the sum is its corresponding weight. The setting of weights for links are the same to the method for nodes. Define the variance of nodes involving geographic location, load capacity, traffic rating, node failure rate, and connectivity as vn_i ($i \in [1, 5]$) respectively, and the variance of links involving the link distance, OSNR, link failure rate, and bandwidth utilization rate correspond to vl_j ($j \in [1, 4]$). The calculation of weights based on variance is shown in (15) and (16). The greater the variance of a parameter, the greater its volatility in the network, indicating that it has a bigger impact on the network state. Thus, parameters with higher

TABLE II
LEVEL AND EVALUATION OF THE NODE i

| Color | Level | Evaluation |
|--------|-----------|----------------------|
| Blue | Excellent | $En_i \in [92, 100]$ |
| Green | Good | $En_i \in [84, 92]$ |
| Yellow | Ordinary | $En_i \in [76, 84]$ |
| Purple | Bad | $En_i \in [68, 76]$ |
| Red | Worse | $En_i \in [60, 68]$ |

TABLE III
LEVEL AND EVALUATION OF THE LINK k

| Color | Level | Evaluation |
|--------|-----------|----------------------|
| Blue | Excellent | $En_i \in [90, 100]$ |
| Green | Good | $En_i \in [80, 90]$ |
| Yellow | Normal | $En_i \in [70, 80]$ |
| Purple | Bad | $En_i \in [60, 70]$ |

variance are given larger weights. This method of setting weights is common and feasible. In addition, five parameters of nodes and four parameters of links only serve as intermediate variables for evaluation and the reference for routing computation, rather than optimal object. In fact, the optimal object is to select nodes and links with the maximum evaluation hop by hop during routing computation, and further improve the performance of routing computation.

$$w_i = \frac{vn_i}{\sum_{i=1}^5 vn_i} \quad (15)$$

$$\alpha_j = \frac{vl_j}{\sum_{j=1}^4 vl_j} \quad (16)$$

All evaluation of nodes and links above are obtained in grades. All the evaluation of nodes are evenly divided into five levels (excellent, good, ordinary, bad, and worse), and the links are evenly divided into four levels (excellent, good, normal, and bad). Different colors indicate different levels of nodes and link in the NTP, as shown in Tables II and III.

For example, the node colored blue and red represent the level of “excellent” and “worse,” respectively, corresponding to evaluations in [92,100] and [60,68]. The link colored blue and red represent the level of “excellent” and “bad,” respectively, corresponding to the evaluations in [90,100] and [60,70].

The graphic description and parameter modeling of NTP have been addressed. The following section discusses the routing calculation based on NTP.

D. Routing Methods and Algorithms

Here, six types of routing algorithms are selected to verify the performance of NTP, namely Dijkstra algorithm [38], Bellman-Ford algorithm [39], the shortest path faster algorithm (SPFA) [40], k shortest paths algorithm (KSP) based on Yen’s [41], A-star (A*) algorithm [42], and branch and bound method [43]. Combined with the routing algorithms, the static and

dynamic routing computation scenarios are used mainly for verification, involving a single path and the k shortest paths.

First, during the process of routing computation, assume that the number of nodes and links resulting from one of the paths is n_{sum} and l_{sum} , respectively. n_i ($i \in [1, n_{sum}]$) and l_j ($j \in [1, l_{sum}]$) correspond to the serial number of a node and link, respectively, during the process of routing computation, and the set of n_i and l_j are N_P and L_P , respectively. The evaluation of this path is defined as E_P . The information of the path including each node, each link, and the evaluation in the path is represented by the matrix P , as shown in (17).

$$P = [N_P, L_P, E_P] \quad (17)$$

The calculation formula for the evaluations of the path is shown in (18), which also considers the relationship between the evaluation and the average number of hops [44].

$$E_P = \frac{1}{n_{sum}} \sum_{m=1}^{n_{sum}} En_m + \frac{1}{l_{sum}} \sum_{n=1}^{l_{sum}} El_n \quad (18)$$

Similarly, the time of routing computation is defined as TR . The method of routing computation based on the NTP is described in detail in Algorithm 1.

Comparing the traditional routing with the routing computation based on NTP, it is not hard to see that the traditional routing computation is the method of solving the shortest path hop by hop, which ignores the influence of the change of network state on the process of routing. For example, at a certain point in time, some nodes or links are faulty or their services are overloaded, and further cannot normally provide the functions of service transmission. However, algorithm 1 shows the process of solving the paths with maximum sum of evaluation for nodes and links hop by hop. Based on NTP, we uniformly transform the performance indicators of nodes and links in the topology into evaluations by means of data normalization and linear weighting. The nodes or links with higher evaluation indicates better performance during service transmission, for example, lower failure rate or stronger load capacity. Therefore, they will be selected preferentially in the routing computation. As mentioned above, a considerable number of nodes and links with poor performance will be avoided in advance, and further improving the performance of routing in the dynamic network scenarios. After obtaining the path by the maximum evaluation by hop, the values of all nodes and links on the path are added up. Considering that only summing the evaluation of nodes and links may results in higher evaluation with the increasing of the number of nodes and links, the hops are taken into account in order to ensure the rationality of comprehensive evaluation of the obtained results based on both the number of hops and path length.

E. Monitoring and Feedback System

To realize dynamic monitoring and feedback between network topology and NTP, a dynamic and real-time feedback system is proposed here. Combined with routing computation, assume that the interval for refreshing network resources and the time of routing computation are T_f and T_R , respectively. The

Algorithm 1: Routing Method Based on NTP.

Input: The source node n_s ; The destination node n_d ;
Output: The path P ;

- 1: Let n_i and l_{n_i, n_j} ($n_i, n_j \in [n_s, n_d]$) be the label of the node i and the link between the node i and the node j , respectively;
- 2: Define En and El as the sum of evaluation for the nodes and links in the path P ;
- 3: Define en_i and el_{n_i, n_j} as intermediate evaluation of the node i and the link between the node i and the node j ;
- 4: Initialize the $\{n_i, l_{n_i, n_j}, N_P, L_P, En, El, E_P\}$;
- 5: **while** $n_i \neq n_d$, update routing table $\{n_i, l_{n_i, n_j}, N_P, L_P, En, El, E_P\}$ by hop;
- 6: **do**
- 7: Finding the maximum value of the sum of en_i , en_j and el_{n_i, n_j} ;
- 8: Getting the nodes n_i and n_j , and the link l_{n_i, n_j} , corresponding to the maximum value;
- 11: Update $N_P = \{n_s, \dots, n_i, \dots, n_d\}$;
- 12: Update $L_P = \{l_{n_s, \dots, n_i}, \dots, l_{n_i, n_j}, \dots, l_{n_j, n_d}\}$;
- 13: $En \leftarrow \sum_{n_s}^{n_i} en_i, El \leftarrow \sum_{l_{n_i, n_j}} el_{n_i, n_j}$;
- 14: Refreshing nodes and links based on the next hop,
- 15: update $n_i, n_j, n_{sum}, l_{sum}$ and l_{n_i, n_j} ;
- 16: **end**
- 17: $E_P = \frac{En}{n_{sum}} + \frac{El}{l_{sum}}$, update P ;
- 18: **return** The path P ;

identity of the state is defined as f_T . The relationship among the three is shown in (19).

$$f_T = \begin{cases} 0, & \text{if } T_R \leq T_f \\ 1, & \text{if } T_R > T_f \end{cases} \quad (19)$$

Here, $f_T = 1$ indicates the change in network resources during routing computation. In this case, a new routing computation needs to be initiated based on the updated parameters. The segments of the path that are different from the previous results are overridden, as shown in Fig. 5. After the replacement of the result for routing computation, the value of f_T reverts to 0. Otherwise, $f_T = 0$ indicates that the previous results of routing computation will be directly reserved.

In the five sections above, the construction of NTP combined with routing computation has been completed. Next, the simulation of NTP and the performance of routing computation are described below.

III. DEMONSTRATION AND RESULTS

The evaluation of nodes and links can be provided based on the construction of the NTP in previous parts. In this part, the simulation about the NTP and routing computation based on NTP are implemented with MATLAB and Visual Studio via interactive functions, which can be divided into two parts: the simulation of NTP and the performance of NTP in routing computation. The simulation setup and results are illustrated as follows.

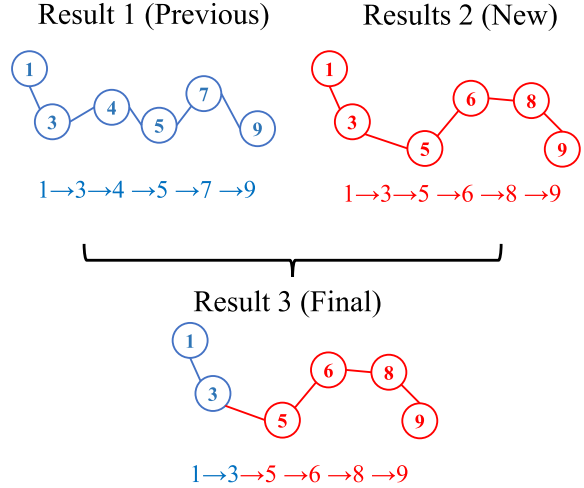


Fig. 5. Replacement process of the results of path computation in dynamic routing computation.

A. Simulation of NTP

The simulation results of NTP include the discriminability for the NTP based on four methods (Min-Max standardization, ratio method, log normalization and trigonometric normalization) of data normalization, the visualized results of NTP based on NSFNET [45] with 14 nodes and CERNET [46] with 38 nodes, the discriminability for the NTP based on Min-Max standardization under different network topologies, and the construction time of NTP with the increasing scales of network topology. The discriminability for the NTP describes the clarity of the NTP after data normalization and linear weighting. Different data normalization and network topologies with different scales both affect this indicator. The parameters of nodes and links are set as follows. Connectivity implies the number of links on a node. Load capacity considers the maximum of service of a node. The traffic rating is influenced by the single-wavelength rates (100 Gbit/s, 200 Gbit/s, 400 Gbit/s, and 800 Gbit/s), corresponding to four levels mentioned before. Geographic location refers to the measured distance between a node and the center of the topology, the larger the measured distance, the smaller the value of geographic location. Link distance is the linear distance between any two nodes, and the transmission loss is directly proportional to the link distance, and the scaling factor is 0.2. Bandwidth utilization rates are a random number between 30% and 80%. OSNR is a random number from 10 dB to 30 dB which is closely related to the link length and amplifier amount. Node failure rate and link failure rate are random numbers among 0-10%. When the value is less than 1%, it is approximate to 0. The weight values for parameters of nodes and links are preset to be equal, satisfying $w_i = 0.2$ ($i \in [1, 5]$) and $\alpha_j = 0.25$ ($i \in [1, 4]$). The simulation platform is based on MATLAB, and the raw data and the computed results from nodes and links are derived from matrix storage and operation respectively. The visualization results of NTP are achieved through the graphical user interface (GUI) of MATLAB. Based on the network topology, the evaluation of nodes and links at different evaluation grades are marked with corresponding color labels.

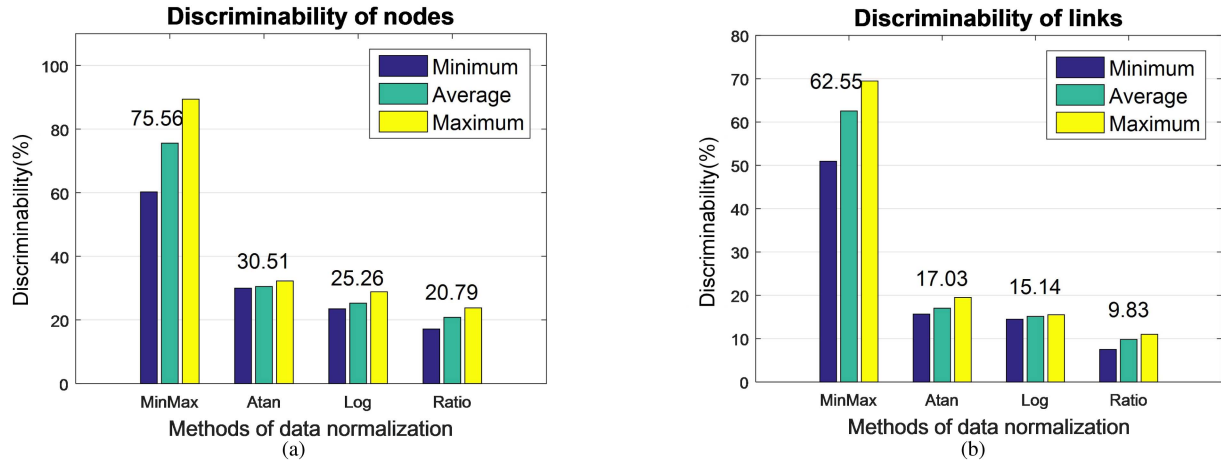


Fig. 6. Discriminability for nodes and links based on the network topology named CERNET with 38 nodes and 100 links. (a) Discriminability of nodes. (b) Discriminability of links.

First, to select the best method for the description of NTP, the network topology named CERNET with 38 nodes are considered. The discriminability for the four methods (Min-Max standardization, ratio method, log normalization and trigonometric normalization) of data normalization at a certain time is verified based on the CERNET. The higher the discriminability, the clearer is the descriptions of NTP, and more clearly the DTOM reproduces the network scenarios in digital space. The calculation formula of the discriminability for the evaluation of nodes and links in NTP is defined as D_s , as shown in (20).

$$D_s = \frac{2(Ev_{\max} - Ev_{\min})}{Ev_{\max}} \times 100\% \quad (20)$$

Here, Ev_{\max} and Ev_{\min} represent the maximum and minimum of evaluation of nodes or links, respectively.

For each method, we conducted 1000 simulation tests on NTP, and selected the maximum, minimum and average values of the discriminability. As shown in Fig. 6, for the discriminability of nodes, the mean value of discriminability under four methods of data normalization are 75.56%, 30.51%, 25.26%, and 20.79%, corresponding to Min-Max standardization, ratio method, log normalization, and trigonometric normalization. Meanwhile, for the discriminability of links, the mean value of discriminability under four methods are 62.55%, 17.03%, 15.14%, and 9.83%. The discriminability of links is less than that of nodes because the number of links in CERNET is more than that of nodes. From the comparison of discriminability, it can be seen the discriminability of the NTP under Min-Max standardization is optimal among the four methods. The clarity under nonlinear normalization involving log normalization and trigonometric normalization is poor, the reason is that the discriminability is small under the two methods when dealing with the large evaluations. For ratio method, because converting the data to ratio reduces the span of the data set, the discriminability is weaken. Compared with ratio method, the span of the data set under Min-Max standardization remains valid. Meanwhile, Min-Max standardization has no disadvantages mentioned in log normalization and trigonometric normalization. Therefore,

Min-Max standardization is finally selected for describing NTP in the following parts.

To describe NTP vividly and clearly, three different network topologies with 14 nodes, 38 nodes and 98 nodes are selected, namely NSFNET, CERNET and the topology extended by CERNET. In this work, considering the clarity of simulation results, the visualized results of NTP based on NSFNET and CERNET are displayed as Figs. 7 and 8. The weighting factors for nodes and links in NTP based on NSFNET and CERNET are both preset to be the same, satisfying $w_i = 0.2$ ($i \in [1, 5]$) and $\alpha_j = 0.25$ ($j \in [1, 4]$). The weights w_i and α_j are not constant and will be further determined by the variances vn_i ($i \in [1, 5]$) and vl_j ($j \in [1, 4]$). As Figs. 7 and 8, the visualized results of NTP at a certain moment based on NSFNET and CERNET are presented. In Fig. 7, the weights of nodes for NTP based on NSFNET satisfy $w_1 = 0.185$, $w_2 = 0.231$, $w_3 = 0.245$, $w_4 = 0.178$ and $w_5 = 0.161$, and the weights of links satisfy $\alpha_1 = 0.245$, $\alpha_2 = 0.221$, $\alpha_3 = 0.147$ and $\alpha_4 = 0.387$. In Fig. 8, the weights of nodes for NTP based on CERNET satisfy $w_1 = 0.102$, $w_2 = 0.144$, $w_3 = 0.267$, $w_4 = 0.298$ and $w_5 = 0.189$, and the weights of links satisfy $\alpha_1 = 0.324$, $\alpha_2 = 0.176$, $\alpha_3 = 0.199$ and $\alpha_4 = 0.301$.

As Figs. 7(a) and 8(a), based on NSFNET and CERNET respectively, the original topology is compared with the topology portrait. Different colors of nodes and links in the topology portrait correspond to different evaluations and levels. The evaluation of nodes and links are shown in Figs. 7(b) and 8(b). The distribution of evaluation with different colors corresponding to different evaluation levels are shown in Figs. 7(c) and 8(c). The evaluations and the proportion of levels of nodes and links are represented by a bar chart and pie chart, respectively, vividly describing the network topology in the form of NTP. The simulation results prove that the methods of describing the network topology in the form of NTP are well-defined and effective. According to topology portraits in Figs. 7 and 8, it is concluded that NTP satisfies the requirement for establishing virtual twins for the network topology in DTOM.

Next, under the network topologies above, the degree of discriminability and its stability based on Min-Max standardization

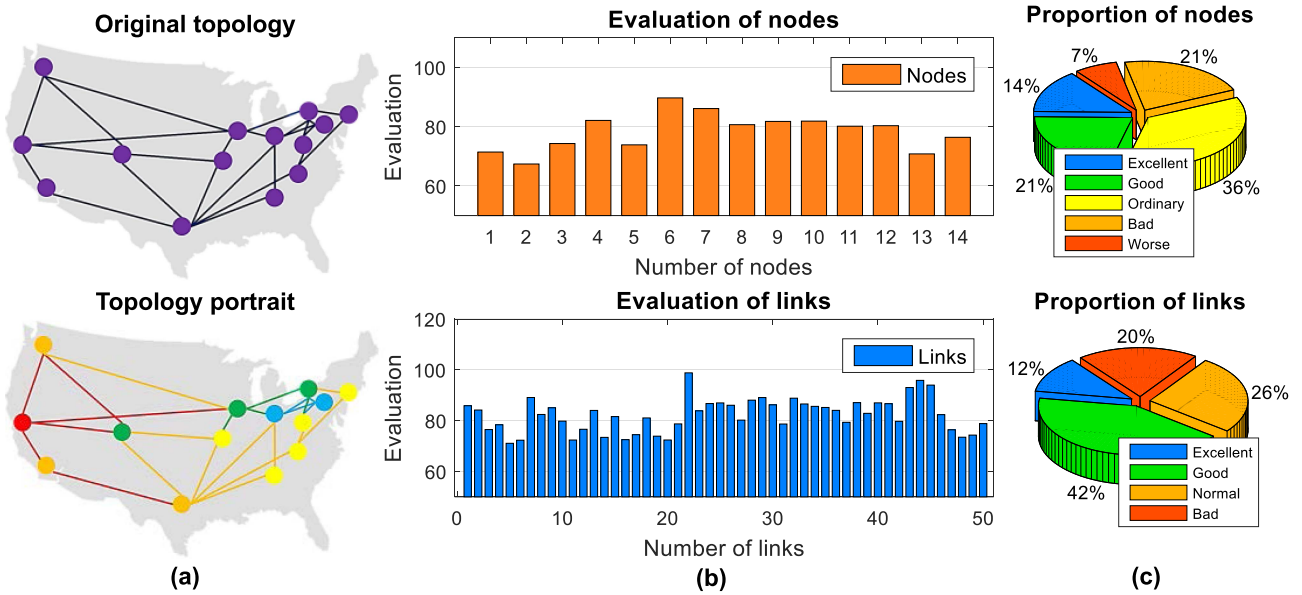


Fig. 7. The visualized results of NTP at a certain moment based on NSFNET with 14 nodes: (a) the original network topology and its topology portrait; (b) evaluation scores of each node and link; (c) proportion of different levels based on evaluation of nodes and links.

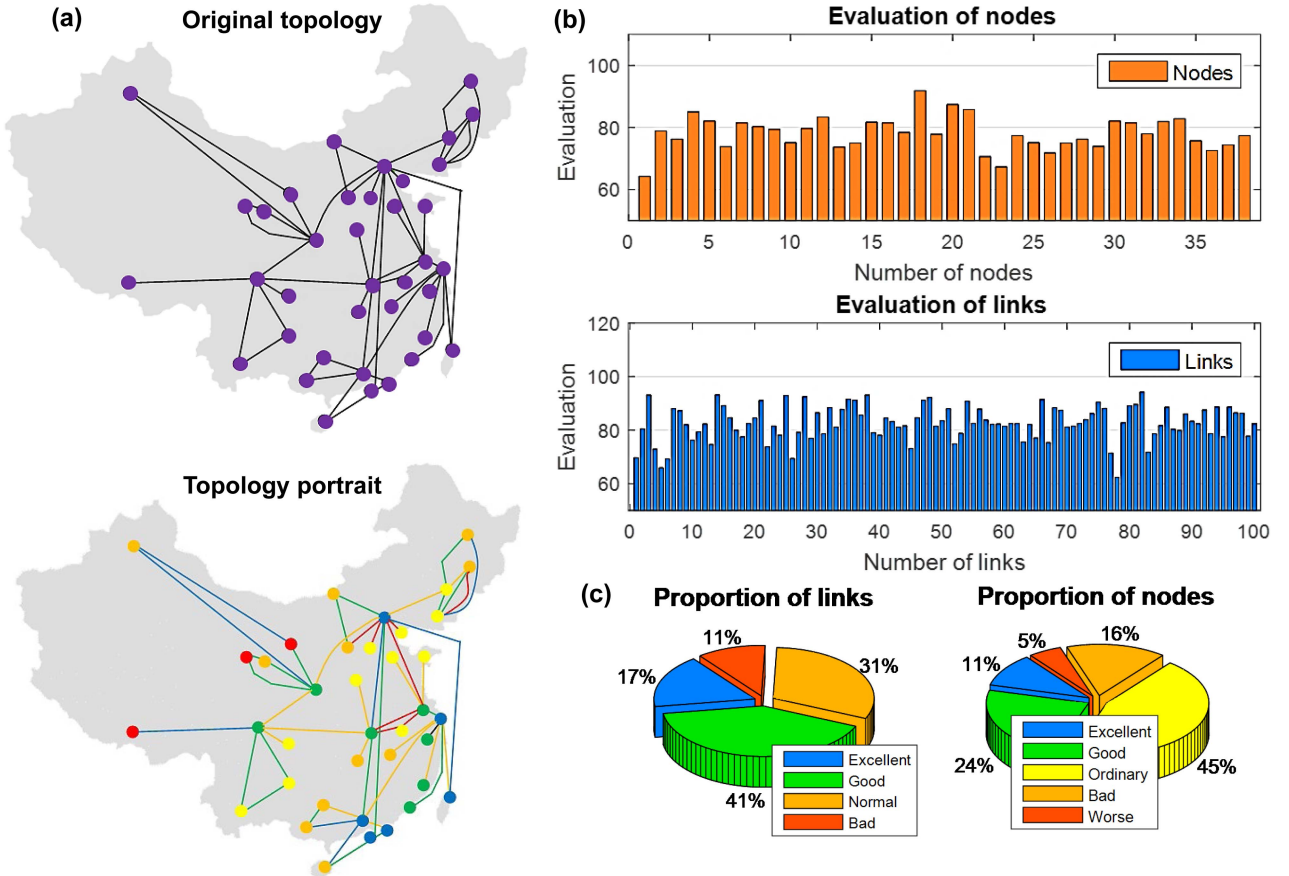


Fig. 8. The visualized results of NTP at a certain moment based on CERNET with 38 nodes: (a) the original network topology and its topology portrait; (b) evaluation scores of each node and link; (c) proportion of different levels based on evaluation of nodes and links.

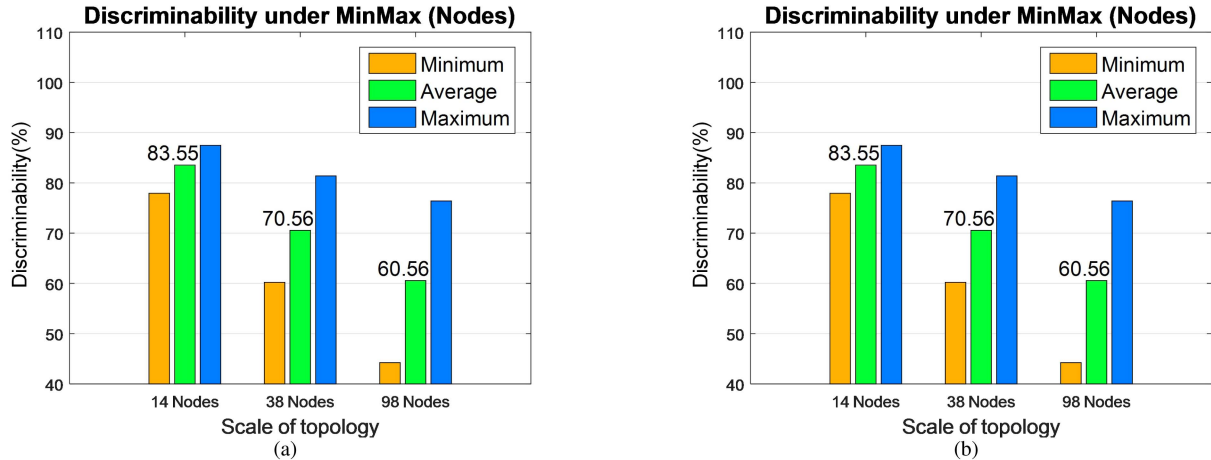


Fig. 9. Discriminability of nodes and links under Min-Max for different scales of network topology. (a) Discriminability of nodes under Min-Max. (b) Discriminability of links under Min-Max.

for NTP are verified as Fig. 9. For each network topology, we conducted 1000 simulation tests on NTP, and selected the maximum, minimum and average values of the discriminability. Discriminability of nodes and links are shown in Fig. 9(a) and (b), respectively. The mean value of discriminability for nodes and links are 83.55% and 75.55%, respectively, for NTP with NSFNET. For NTP with CERNET, the mean value of discriminability of nodes and links are 70.56% and 62.55%, respectively. For NTP with 98 nodes, the average of discriminability of nodes and links correspond to 60.56% and 50.14%, respectively. Based on Min-Max standardization, the discriminability of nodes and links under the three scales can maintain an acceptable level.

The discriminability of NTP decreases with the increasing scale of network topology. It is related to the fact that the number of nodes and links increases with the growth of the scale of network topology in a fixed evaluation interval. For the stability, with the increasing of the scale for network topology, the fluctuation of the discriminability between its minimum and maximum increases. For example, for Min-Max, the fluctuation ratio of the discriminability under the network topology with 14, 38, and 98 nodes are 10%, 19%, and 28%, respectively. Nevertheless, the mean value of the discriminability is closer to its maximum, proving that the discriminability can remain acceptable in most cases.

To test the construction time for NTP, the network topology with the scales from 14 nodes to 98 nodes are selected. The times of simulation in each network topology is 1000, and construction time in Fig. 10 derives from the mean value based on the simulation. The result of the construction time for NTP is shown in Fig. 10. The construction time for NTP increases linearly with the increase in the scales of the network topology. The construction time for NTP with 14 nodes and 98 nodes corresponds to 2.6 ms and 11.4 ms, indicating that the construction time is reasonable and acceptable even for the large-scale network topology. The time cost mainly comes from the construction process of the NTP and the calculation process of the evaluation of nodes and links.

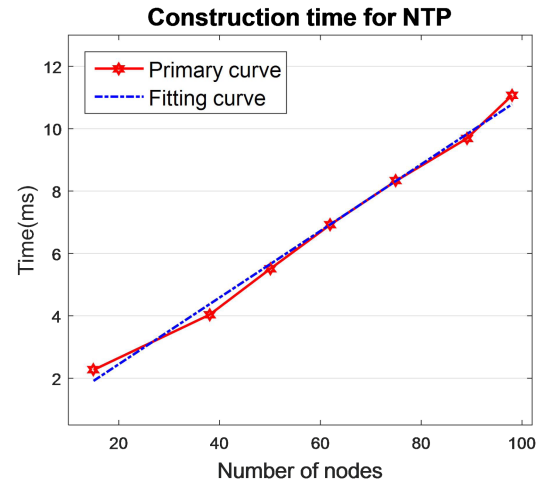
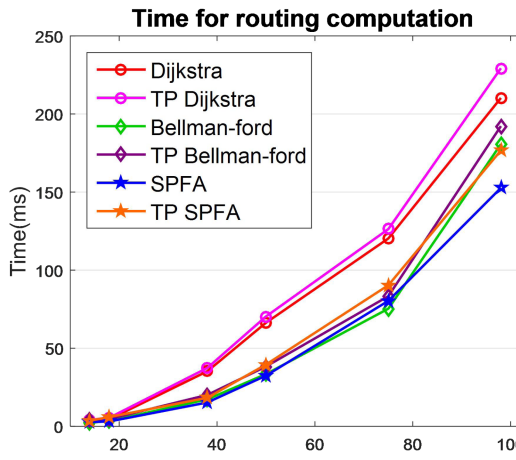


Fig. 10. Construction time of NTP with the increasing scales of network topology.

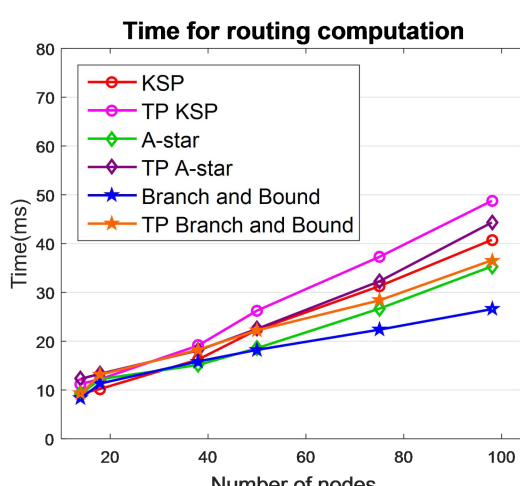
Therefore, in this section, it is concluded that the methods of describing the network topology in the form of NTP based on Min-Max standardization are effective. The construction time for NTP increases linearly with the increase of the scale of the network topology that additionally indicates that the mode of construction is reasonable and acceptable even for the large-scale network topology.

B. Routing Computation in Dynamic Scenes

To investigate the advantages of NTP in DTOM, in this section, the performance of routing computation in dynamic scenes based on NTP is verified, involving time for routing computation, outage probability, outage latency, and the number of services requests. Each validation and the associated routing algorithms from the four sections are shown in detail as follows. The network topologies includes 14 nodes, 18 nodes, 38 nodes, 57 nodes, 75 nodes, and 98 nodes, involving NSFNET, CERNET, and some self-designed network topologies. Six



(a) First set of algorithms: Dijkstra, Bellman-Ford, and SPFA.



(b) Second set of algorithms, KSP, A*, and Branch and Bound.

Fig. 11. Time for routing computation with the increase of the scales of network topology.

routing algorithms named Dijkstra, Bellman-Ford, SPFA, KSP algorithm based on Yen's, A* algorithm, and the branch and bound method are selected to verify the performance of routing computation based on NTP. The six algorithms above are divided into two types, respectively corresponding to traditional routing algorithms and the improved routing algorithms. First set of routing algorithms named traditional routing algorithms includes Dijkstra, Bellman-Ford and SPFA. The second set of routing algorithms named the improved routing algorithms involves KSP algorithm based on Yen's, A* algorithm, and the branch and bound method. The improved routing algorithms are derived from the heuristic improvement of the traditional routing algorithm.

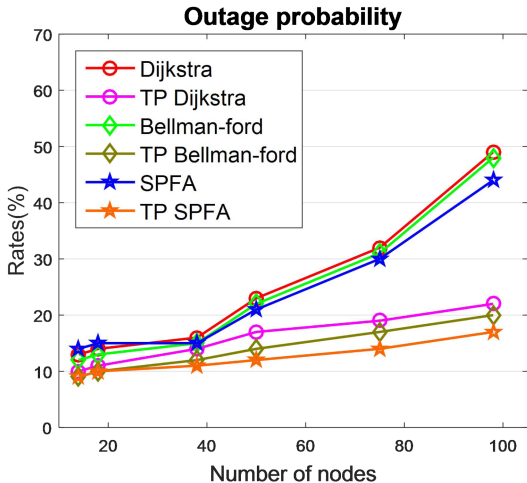
For the time for routing computation, outage probability and outage latency, the conditions of comparing all above algorithms are shown as follows. First, the times of simulation with each algorithm in each network topology is 1000. For each network topology, 10 different pairs of source and destination nodes are selected. All of the data from Figs. 11 to 13 are from the mean value of the simulations. The construction process of

NTP follows the previous section. The evaluations of nodes and links are generated by Min-Max standardization and linear weighting. During routing computation, the type of services transmitted, the number of users, and the type of users are the same. Meanwhile, the simulation platform is based on the joint programming of MATLAB and Visual Studio. Based on the NTP, the sum of link distance in routing computation is replaced by the weighted average of comprehensive evaluation from node and link evaluation. The evaluation computed by MATLAB are all passed to Visual Studio via interactive functions in the form of a numerical matrix for routing computation. The routing algorithms mentioned above are supported by the standard library and the functions to describe the graph involving vectors and mapping come from source files and header files based on Visual Studio, and are further modified to be compatible with the simulation results of NTP in MATLAB. All simulation results are shown as follows. Meanwhile, TP means routing algorithms combined with NTP. Both TP and NTP in the legend of simulation results represent routing algorithms based on the evaluation of the topology portrait.

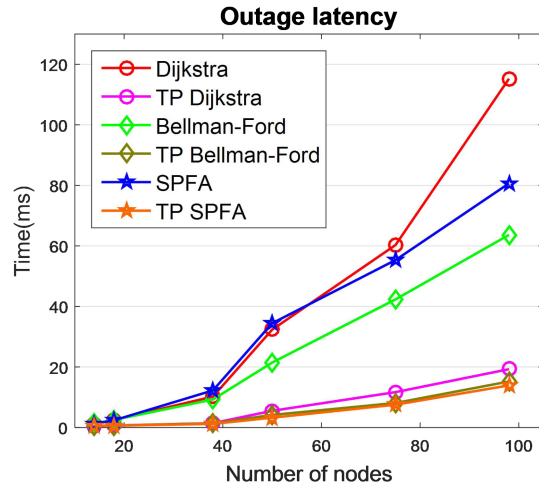
First, considering the time for routing computation, as the scale of the network topology increases, we compared the performance of the same routing algorithm combined with NTP with the algorithm without NTP, corresponding to Fig. 11. Based on the classification of routing algorithm (involving traditional routing algorithm and improved routing algorithm based on heuristics), the simulation results are divided into two types as Fig. 11(a) and (b).

From Fig. 11(a), it is observed that compared with routing computation without NTP, when the number of nodes is less than or equal to 20, the time of routing computation combined with NTP under the routing algorithms (Dijkstra, Bellman-Ford, and SPFA) increases from 1 ms to 3 ms. When the number of nodes is greater than 20, the time of routing computation increases from 10 ms to 18 ms and tends to stay fixed. Considering the topology with 98 nodes as an example, the time of routing computation under routing algorithm Dijkstra increases from 210 ms to 226 ms. From Fig. 11(b), we can draw similar conclusions under routing algorithms namely KSP based on Yen's, A-star, and Branch and Bound. The only difference is that the time cost of NTP varies from 8 ms to 15 ms. Because the evaluation of nodes and links needs to be calculated before implementing the routing algorithms, the time of routing computation will be increased to a certain extent, but the increment is slight. Therefore, it is proved that the topology portrait provides additional, but acceptable and stable time cost for routing computation. Due to the time and space complexity of the routing algorithms, the methods of evaluation for global data cannot reduce the time cost of routing computation. Otherwise, multi-factor evaluation may improve the performance of routing computation in other aspects.

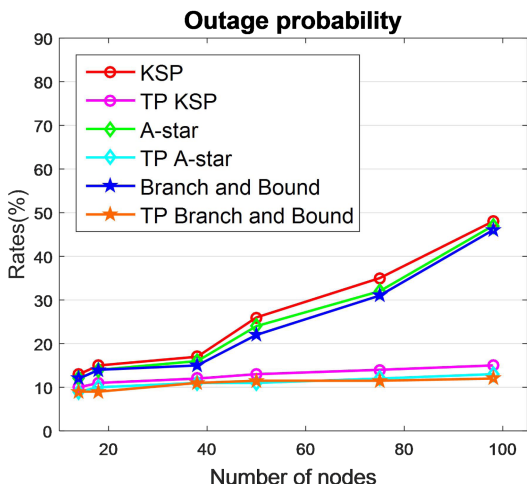
In dynamic scenarios, routing computation may be interrupted owing to the faults from nodes or links at a certain time because of the dynamically refreshing parameters of nodes and links in topology. Therefore, the outage probability and outage latency have been introduced to verify the stability of the NTP. The simulation results are provided in detail, as summarized in Figs. 12 and 13.



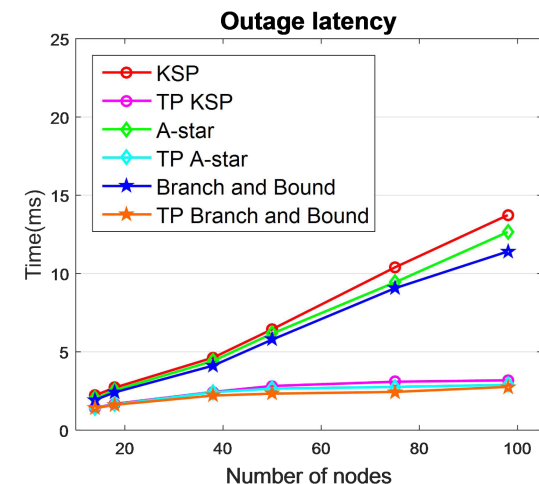
(a) First set of algorithms: Dijkstra, Bellman-Ford, and SPFA.



(a) First set of algorithms: Dijkstra, Bellman-Ford, and SPFA.



(b) Second set of algorithms: KSP, A*, and Branch and Bound.



(b) Second set of algorithms: KSP, A*, and Branch and Bound.

Fig. 12. Outage probability with the increase of the scales of network topology.

Fig. 13. Outage latency with the increase in the scales of network topology.

From Figs. 12 and 13, the outage probability and outage latency without NTP increase significantly for the six routing algorithms owing to dynamic changes in the network parameters. For the outage probability in Fig. 12, the growth rate of outage probability of dynamic routing computation based on NTP slows down significantly as the scale of network topology increases. Considering the routing algorithms Dijkstra and KSP based on Yen's from Fig. 12(a) and (b) as examples, compared with the routing computation under dynamic scenes without NTP, the outage probability with NTP decreases from 49% and 48% to 21% and 15%, respectively, under the network topology with 98 nodes. For the outage latency shown in Fig. 13, under the same network topology with 98 nodes and the same routing algorithms, compared with the routing computation under dynamic scenes without NTP, the outage latency with NTP decrease from 116 ms and 16.9 ms to 20 ms and 3 ms. Generally speaking, the traditional routing computation ignores the influence of the change of network state. However, in NTP, the performance parameters of nodes and links representing the network state are uniformly transformed into evaluations

through data normalization and linear weighting. The nodes or links with higher evaluation indicates better performance during service transmission, for example, lower failure rate or stronger load capacity. They will be selected preferentially in the routing computation. As mentioned above, a considerable number of nodes and links with poor performance will be avoided in advance to reduce unnecessary time cost in service transmission under dynamic network scenarios. Accordingly, it may be concluded that owing to multi-factor evaluation for nodes and links, the routing computation in dynamic scenes avoids a considerable number of nodes and links with low evaluation, thereby improve the communication quality, specifically avoiding the nodes and links with lower performance, and further reduces the outage probability and outage latency.

Finally, from Figs. 14 to 16, for the number of service requests per minute, one path selected by routing computation corresponds to one transmitted service. The services transmitted in different network topologies are the same type, The number of users are the same, and the type of users are the same. Similarly, 10 pairs of source and destination nodes are selected. Based

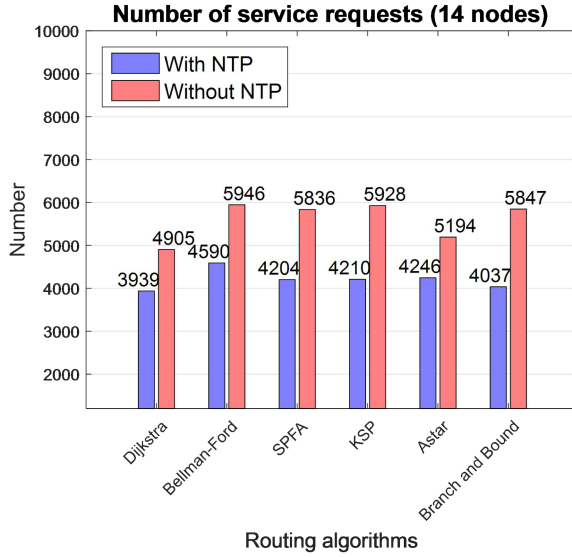


Fig. 14. Number of service requests per minute from the same source node to the destination node for the NTP with 14 nodes.

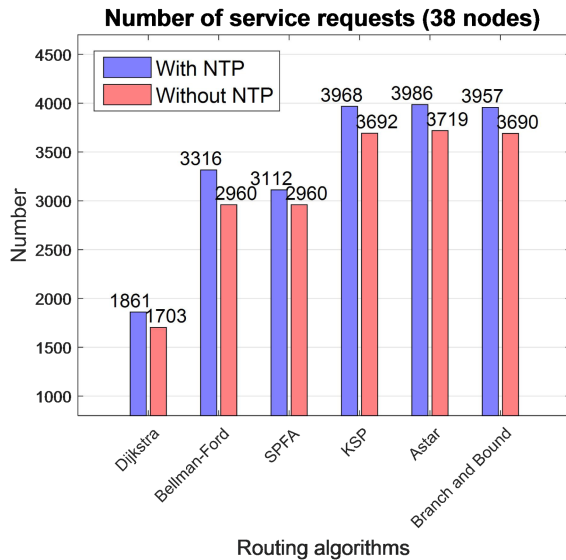


Fig. 15. Number of service requests per minute from the same source node to the destination node for the NTP with 38 nodes.

on different network topology, the numbers of simulation with each pair of nodes under each routing algorithm is 1000. All of the data from Figs. 14 to 16 are the mean value. In addition, the evaluation of nodes and links are generated in the same way through Min-Max data normalization and linear weighting. The number of service requests per minute from the same source node to the same destination node under the network topology with 14, 38, and 98 nodes are measured. In addition, the simulation platform is the same as the previous three tests.

From Fig. 14, under the NTP with 14 nodes, the number of service requests with NTP is less than the number without NTP. However, from Figs. 15 and 16, the number of service requests with NTP is improved. Considering the routing algorithm Dijkstra as an example, compared with the number of service requests

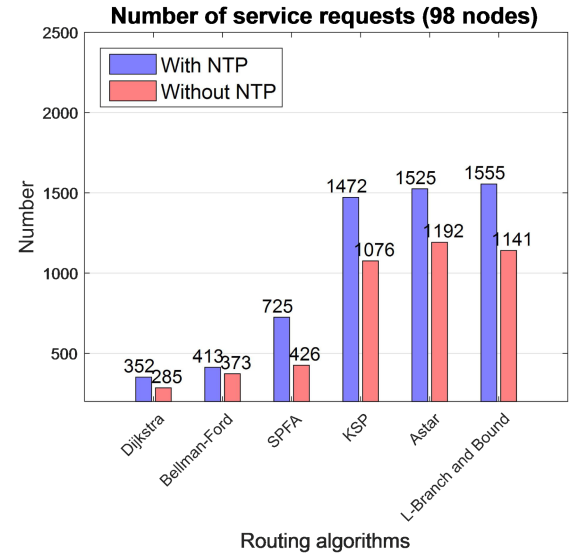


Fig. 16. Number of service requests per minute from the same source node to the destination node for the NTP with 98 nodes.

without NTP, the number for the NTP with 38 and 98 nodes is increased by 9.2% and 23.3%, respectively. For the other routing algorithms under the same conditions, the number increase by 9% and 20% to 15% and 30%, respectively, for the NTP with 38 and 98 nodes, indicating that the larger the scale of the network topology, the greater improvement is achieved in the growth rate of the number of service requests. In dynamic network scenarios, because of reducing the time cost by avoiding nodes and links with lower evaluation (lower performance), the time cost of routing are reduced, and further improve the performance of the number of service requests. Accordingly, it is proved that the routing algorithm based on multi-factor evaluation for nodes and links in NTP also effectively improves the number of service requests, especially under the larger network topology.

Accordingly, it is concluded that the NTP improves the performance of dynamic routing computation in outage probability, outage latency, and the number of service requests.

Overall, it is proved that due to the multi-factor evaluation of the NTP, the time for routing computation is increased within an acceptable range. However, the other performance metrics of routing computation, namely, the outage probability, outage latency, and the number of service requests are significantly improved. Although the generation of evaluation brings a little bit time cost, a considerable number of nodes and links with poor performance will be avoided in advance to reduce unnecessary outage probability and latency in service transmission under dynamic network scenarios. Accordingly, based on NTP, it is concluded that based on NTP, the time for routing computation is sacrificed a little bit time cost in exchange for significantly improvements in the other performance involving outage probability, outage latency, and the number of service requests. Finally, it is further proved that NTP in DTOM can improve the performance of the network.

IV. CONCLUSION

This paper proposed a multi-factor NTP for DTON. All the parameters of nodes and links in the topology were unified in dimension and transformed into equivalent values by data normalization. Subsequently, they were transformed into the evaluation by linear weighting in order to achieve the comprehensive description for the network topology. Meanwhile, combined with dynamic scenes in routing computation, further validation for the performance of the NTP was provided. The main conclusions drawn in this study were as follows.

First, for the generation methods for NTP, various factors were evaluated based on four methods of data normalization: Min-Max standardization, ratio method, log normalization and trigonometric normalization. Through the results, it was proved that the Min-Max standardization exhibits a higher degree of discriminability compared with the other three methods. And for the Min-Max standardization, the discriminability under different scales of network topology was verified. Among them, two different NTPs, referred to as NSFNET and CERNET, were simulated. It was concluded that even in the larger network topology, the discriminability of the NTP under Min-Max standardization remained substantial, and as the scales of the topology increased, the construction time became more acceptable and reasonable. Finally, for the performance of routing computation under the NTP, considering six different routing algorithms (Dijkstra, SPFA, Bellman-Ford, KSP based on Yen's, A*, and the branch and bound method) in the routing computation time, the indicator was increased owing to the time cost of the evaluation, proving that the NTP inevitably resulted in a certain time cost that was acceptable. Furthermore, the performance of the other three parts was improved by the NTP, indicating that the methods of evaluation could provide preplans and avoid the nodes or links with low quality in advance, thus improving the performance of outage probability and outage latency, and further increasing the number of service requests in dynamic scenes. Therefore, the NTP improved the performance of routing computation and further provided a substantial scheme for improving the network performance of DTON.

REFERENCES

- [1] F. Tao, Q. Qi, and L. Wang, "Digital twins and cyber-physical systems toward smart manufacturing and industry 4.0: Correlation and comparison," *Engineering*, vol. 5, no. 4, pp. 653–611, Aug. 2019, doi: [10.1109/J.ENG.2019.01.014](https://doi.org/10.1109/J.ENG.2019.01.014).
- [2] H. X. Nguyen, R. Trestian, D. To, and M. Tatipamula, "Digital twin for 5G and beyond," *IEEE Commun. Mag.*, vol. 59, no. 2, pp. 10–15, Feb. 2021, doi: [10.1109/MCOM.001.2000343](https://doi.org/10.1109/MCOM.001.2000343).
- [3] D. Wang et al., "The role of digital twin in optical communication: Fault management, hardware configuration, and transmission simulation," *IEEE Commun. Mag.*, vol. 59, no. 1, pp. 133–139, Jan. 2021, doi: [10.1109/MCOM.001.2000727](https://doi.org/10.1109/MCOM.001.2000727).
- [4] R. Vilalta, R. Casellas, L. Gifre, R. Muñoz, and R. Martínez, "Architecture to deploy and operate a digital twin optical network," in *Proc. Opt. Fiber Commun. Conf. Exhib.*, 2022, pp. 1–3.
- [5] K. S. Mayer, J. A. Soares, R. P. Pinto, C. E. Rothenberg, D. S. Arantes, and D. A. A. Mello, "Machine-learning-based soft-failure localization with partial software-defined networking telemetry," *IEEE J. Opt. Commun. Netw.*, vol. 13, no. 10, pp. E122–E131, Oct. 2021, doi: [10.1364/JOCN.424654](https://doi.org/10.1364/JOCN.424654).
- [6] A. Ferrari, V. V. Garbhupu, D. L. Gac, I. F. de Jauregui Ruiz, G. Charlet, and Y. Pointurie, "Demonstration of AI-Light: An automation framework to optimize the channel powers leveraging a digital twin," in *Proc. Opt. Fiber Commun. Conf. Exhib.*, 2022, pp. 1–3.
- [7] X. Pang et al., "Digital twin-assisted optical power allocation for flexible and customizable SNR optimization," in *Proc. Opt. Fiber Commun. Conf. Exhib.*, 2022, pp. 1–3.
- [8] M. P. Yankov, U. C. de Moura, and F. D. Ros, "Power evolution modeling and optimization of fiber optic communication systems with EDFA repeaters," *IEEE J. Lightw. Technol.*, vol. 39, no. 10, pp. 3154–3161, May 2021, doi: [10.1109/JLT.2021.3061632](https://doi.org/10.1109/JLT.2021.3061632).
- [9] J. Li, D. Wang, and M. Zhang, "Digital twin-enabled self-evolved optical transceiver using deep reinforcement learning," *Opt. Lett.*, vol. 45, no. 16, pp. 4654–4657, 2020, doi: [10.1364/ol.397972](https://doi.org/10.1364/ol.397972).
- [10] Y. Wu, K. Zhang, and Y. Zhang, "Digital twin networks: A survey," *IEEE Internet Things*, vol. 8, no. 18, pp. 13789–13804, Sep. 2021, doi: [10.1109/JIOT.2021.3079510](https://doi.org/10.1109/JIOT.2021.3079510).
- [11] H. Yang, Y. Li, K. Yao, T. Sun, and C. Zhou, "A systematic network traffic emulation framework for digital twin network," *Proc. IEEE 1st Int. Conf. Digit. Twins Parallel Intell.*, 2021, pp. 94–97.
- [12] B. Zhang, J. Zheng, and H. T. Mouftah, "Fast routing algorithms for lightpath establishment in wavelength-routed optical networks," *IEEE J. Lightw. Technol.*, vol. 26, no. 13, pp. 1744–1751, Jul. 2008, doi: [10.1109/JLT.2007.912530](https://doi.org/10.1109/JLT.2007.912530).
- [13] R. R. Reyes and T. Bauschert, "Adaptive and state-dependent online resource allocation in dynamic optical networks," *IEEE J. Opt. Commun. Netw.*, vol. 9, no. 3, pp. B64–B77, Mar. 2017, doi: [10.1364/JOCN.9.000B64](https://doi.org/10.1364/JOCN.9.000B64).
- [14] M. Hadi, M. R. Pakravan, and E. Agrell, "Dynamic resource allocation in metro elastic optical networks using Lyapunov drift optimization," *IEEE J. Opt. Commun. Netw.*, vol. 11, no. 6, pp. 250–259, Jun. 2019, doi: [10.1364/JOCN.11.000250](https://doi.org/10.1364/JOCN.11.000250).
- [15] F. Morales, M. Ruiz, L. Gifre, L. M. Contreras, V. Lopez, and L. Velasco, "Virtual network topology adaptability based on data analytics for traffic prediction," *IEEE J. Opt. Commun. Netw.*, vol. 9, no. 1, pp. A35–A45, Jan. 2017, doi: [10.1364/JOCN.9.000A35](https://doi.org/10.1364/JOCN.9.000A35).
- [16] Z. Zhu, W. Lu, L. Zhang, and N. Ansari, "Dynamic service provisioning in elastic optical networks with hybrid single-/multi-path routing," *IEEE J. Lightw. Technol.*, vol. 31, no. 1, pp. 15–22, Jan. 2013, doi: [10.1109/JLT.2012.2227683](https://doi.org/10.1109/JLT.2012.2227683).
- [17] P. Lu, L. Zhang, X. Liu, J. Yao, and Z. Zhu, "Highly efficient data migration and backup for big data applications in elastic optical inter-data-center networks," *IEEE Netw.*, vol. 29, no. 5, pp. 36–42, Sep./Oct. 2015, doi: [10.1109/MNET.2015.7293303](https://doi.org/10.1109/MNET.2015.7293303).
- [18] J. Liu, W. Lu, F. Zhou, P. Lu, and Z. Zhu, "On dynamic service function chain deployment and readjustment," *IEEE Trans. Netw. Serv. Manage.*, vol. 14, no. 3, pp. 543–553, Sep. 2017, doi: [10.1109/TNSM.2017.2711610](https://doi.org/10.1109/TNSM.2017.2711610).
- [19] C. F. Hsu, Y. C. Chang, and S. C. Sie, "Graph-model-based dynamic routing and spectrum assignment in elastic optical networks," *IEEE J. Opt. Commun. Netw.*, vol. 8, no. 7, pp. 507–520, Jul. 2016, doi: [10.1364/JOCN.8.000507](https://doi.org/10.1364/JOCN.8.000507).
- [20] K. Ishii, A. Takefusa, S. Namiki, and T. Kudoh, "Topology description generation and path computation framework for dynamic optical path network with heterogeneous switches," in *Proc. Opt. Fiber Commun. Conf. Expo.*, 2018, pp. 1–3.
- [21] K. Ishii, A. Takefusa, S. Namiki, and T. Kudoh, "Optical network resource management supporting physical layer reconfiguration," *IEEE J. Lightw. Technol.*, vol. 37, no. 21, pp. 5442–5454, Nov. 2019, doi: [10.1109/JLT.2019.2935789](https://doi.org/10.1109/JLT.2019.2935789).
- [22] Y. Zhao et al., "Low complexity OSNR monitoring and modulation format identification based on binarized neural networks," *IEEE J. Lightw. Technol.*, vol. 38, no. 6, pp. 1314–1322, Mar. 2020, doi: [10.1109/JLT.2020.2973232](https://doi.org/10.1109/JLT.2020.2973232).
- [23] T. Sasai, M. Nakamura, E. Yamazaki, S. Yamamoto, H. Nishizawa, and Y. Kisaka, "Digital backpropagation for optical path monitoring: Loss profile and passband narrowing estimation," in *Proc. Eur. Conf. Opt. Commun.*, 2020, pp. 1–4.
- [24] H. Kim and K. Chung, "Multipath-based HTTP adaptive streaming scheme for the 5G network," *IEEE Access*, vol. 8, pp. 208809–208825, 2020, doi: [10.1109/ACCESS.2020.3038854](https://doi.org/10.1109/ACCESS.2020.3038854).
- [25] M. Ruiz, F. Coltraro, and L. Velasco, "CURSA-SQ: A methodology for service-centric traffic flow analysis," *IEEE J. Opt. Commun. Netw.*, vol. 10, no. 9, pp. 773–784, Sep. 2018, doi: [10.1364/JOCN.10.000773](https://doi.org/10.1364/JOCN.10.000773).
- [26] H. Son, S. Lee, S.-C. Kim, and Y.-S. Shin, "Soft load balancing over heterogeneous wireless networks," *IEEE Trans. Veh. Technol.*, vol. 57, no. 4, pp. 2632–2638, Jul. 2008, doi: [10.1109/TVT.2007.912324](https://doi.org/10.1109/TVT.2007.912324).
- [27] R. Jin et al., "Detecting node failures in mobile wireless networks: A probabilistic approach," *IEEE Trans. Mobile Comput.*, vol. 15, no. 7, pp. 1647–1660, Jul. 2016, doi: [10.1109/TMC.2015.2474371](https://doi.org/10.1109/TMC.2015.2474371).

- [28] K. N. Georgakilas, K. Katrinis, A. Tzanakaki, and O. B. Madsen, "Performance evaluation of impairment-aware routing under single- and double-link failures," *IEEE J. Opt. Commun. Netw.*, vol. 2, no. 8, pp. 633–641, Aug. 2010, doi: [10.1364/JOCN.2.000633](https://doi.org/10.1364/JOCN.2.000633).
- [29] V. S. Durga and T. Jayaprakash, "An effective data normalization strategy for academic datasets using log values," in *Proc. Int. Conf. Commun. Electron. Syst.*, 2019, pp. 610–612.
- [30] M. Fallah and S. A. Edalatpanah, "On the some new preconditioned generalized AOR methods for solving weighted linear least squares problems," *IEEE Access*, vol. 8, pp. 33196–33201, 2020, doi: [10.1109/ACCESS.2020.2973289](https://doi.org/10.1109/ACCESS.2020.2973289).
- [31] R. Ferrero, M. V. Bueno-Delgado, and F. Gandino, "In- and out-degree distributions of nodes and coverage in random sector graphs," *IEEE Trans. Wireless Commun.*, vol. 13, no. 4, pp. 2074–2085, Apr. 2014, doi: [10.1109/TWC.2014.031314.130905](https://doi.org/10.1109/TWC.2014.031314.130905).
- [32] Z. Feng, Y. Fang, and H. Shi, "Towards large-capacity and intelligent optical transmission systems: Opportunities, challenges, and solutions," *ZTE Technol. J.*, vol. 28, no. 1, pp. 62–69, Feb. 2022, doi: [10.12142/ZTETJ.202201013](https://doi.org/10.12142/ZTETJ.202201013).
- [33] K. Poularakis, J. Llorca, A. M. Tulino, I. Taylor, and L. Tassiulas, "Service placement and request routing in MEC networks with storage, computation, and communication constraints," *IEEE ACM Trans. Netw.*, vol. 28, no. 3, pp. 1047–1060, Jun. 2020, doi: [10.1109/TNET.2020.2980175](https://doi.org/10.1109/TNET.2020.2980175).
- [34] N. Guo, S. K. Bose, B. Mukherjee, and G. Shen, "Impact of fiber attenuation and effective area on spectrum efficiency of elastic optical networks," *J. Lightw. Technol.*, vol. 40, no. 8, pp. 2200–2213, Apr. 2022, doi: [10.1109/JLT.2021.3136574](https://doi.org/10.1109/JLT.2021.3136574).
- [35] X. Guan and K. Jiang, "New way of data normalization for satellite communication network," *J. Comput. Appl.*, vol. 28, no. S2, pp. 230–232, Dec. 2008.
- [36] D. Singh and B. Singh, "Investigating the impact of data normalization on classification performance," *Appl. Soft. Comput.*, vol. 97, pp. 105524–105556, Dec. 2020, doi: [10.1016/j.asoc.2019.105524](https://doi.org/10.1016/j.asoc.2019.105524).
- [37] Y. Yao, Z. Zhang, H. Cui, T. Ren, and J. Xiao, "The influence of student abilities and high school on student growth: A case study of chinese national college entrance exam," *IEEE Access*, vol. 7, pp. 148254–148264, 2019, doi: [10.1109/ACCESS.2019.2946503](https://doi.org/10.1109/ACCESS.2019.2946503).
- [38] I. Szczesniak, A. Jajszczyk, and B. W. Szczesniak, "Generic dijkstra for optical networks," *IEEE J. Opt. Commun. Netw.*, vol. 11, no. 11, pp. 568–577, Nov. 2019, doi: [10.1364/JOCN.11.000568](https://doi.org/10.1364/JOCN.11.000568).
- [39] Y. Mo, S. Dasgupta, and J. Beal, "Robustness of the adaptive Bellman–Ford algorithm: Global stability and ultimate bounds," *IEEE Trans. Autom. Control*, vol. 64, no. 10, pp. 4121–4136, Oct. 2019, doi: [10.1109/TAC.2019.2904239](https://doi.org/10.1109/TAC.2019.2904239).
- [40] X. Yu et al., "Path planning in Multiple-AUV systems for difficult target traveling missions: A hybrid metaheuristic approach," *IEEE Trans. Cogn. Develop. Syst.*, vol. 12, no. 3, pp. 561–574, Sep. 2020, doi: [10.1109/TAC.2019.2904239](https://doi.org/10.1109/TAC.2019.2904239).
- [41] H. Liu, C. Jin, B. Yang, and A. Zhou, "Finding top-k shortest paths with diversity," *IEEE Trans. Knowl. Data. Eng.*, vol. 30, no. 3, pp. 488–502, Mar. 2018, doi: [10.1109/TKDE.2017.2773492](https://doi.org/10.1109/TKDE.2017.2773492).
- [42] Z. Liu, H. Liu, Z. Lu, and Q. Zeng, "A dynamic fusion pathfinding algorithm using delaunay triangulation and improved A-star for mobile robots," *IEEE Access*, vol. 9, pp. 20602–20621, 2021, doi: [10.1109/ACCESS.2021.3055231](https://doi.org/10.1109/ACCESS.2021.3055231).
- [43] K. Cumanan, R. Krishna, L. Musavian, and S. Lambotharan, "Joint beamforming and user maximization techniques for cognitive radio networks based on branch and bound method," *IEEE Trans. Wireless Commun.*, vol. 9, no. 10, pp. 3082–3092, Oct. 2010, doi: [10.1109/TWC.2010.072610.090898](https://doi.org/10.1109/TWC.2010.072610.090898).
- [44] H. V. Madhyastha and N. Balakrishnan, "An efficient algorithm for virtual-wavelength-path routing minimizing average number of hops," *IEEE J. Sel. Areas Commun.*, vol. 21, no. 9, pp. 1433–1440, Nov. 2003, doi: [10.1109/JSAC.2003.818228](https://doi.org/10.1109/JSAC.2003.818228).
- [45] C. L. Triveni, P. C. Srikanth, and T. Srinivas, "An optimized routing algorithm for elastic optical network," in *Proc. Int. Conf. Electr., Electron. Optim. Techn.*, 2016, pp. 3873–3878.
- [46] X. Zhang and X. Li, "Native multicast based videoconference service on CERNET," in *Proc. Int. Conf. Commun. Technol.*, 2006, pp. 1–4.